

Non Classical Rotational Inertia Fraction in a One Dimensional Model of Supersolid

Néstor Sepúlveda¹, Christophe Josserand^{2,3}, and Sergio Rica^{1,4}

¹ *Laboratoire de Physique Statistique de l'Ecole normale supérieure,
24 Rue Lhomond, 75231 Paris Cedex 05, France.*

² *Institut Jean Le Rond D'Alembert, UMR 7190 CNRS-UPMC, 4 place Jussieu, 75005 Paris, France.*

³ *Kavli Institute for Theoretical Physics, University of California, Santa Barbara, CA 93106, USA*

⁴ *Departamento de Física, Universidad de Chile, Blanco Encalada 2008, Santiago, Chile.*

We study the rotational inertia of a model of supersolid in the frame of the mean field Gross-Pitaevskii theory in one space dimension. We discuss the ground state of the model and the existence of a non classical inertia (NCRI) under rotation that models an annular geometry. An explicit formula for the NCRI is deduced. It depends on the density profil of the ground state, in full agreement with former theories. We compare the NCRI computed through this theory with direct numerical simulations of rotating 1D systems.

INTRODUCTION

Since pioneering works by Andreev and Lifshitz[1], Chester[2], Leggett[3] and others, supersolids have been dreamt up as a kind of Bose-Einstein condensation of defects, vacancies or interstitials. They would achieve a coherent state that could allow a matter flow trough the crystal. Although the quest for a supersolid state over the last 40 years has failed[4], the context has totally changed with the recent experiments by Kim and Chan[5–7]. In these experiments, solid Helium⁴ fills a torsional oscillator under small oscillations and the rotational frequency is measured. Surprisingly, the rotational inertia shows a drop below few tenths of Kelvin. This non-classical rotational inertia (NCRI) is believed to be the signature of the transition of a fraction of the solid into a supersolid state. The situation has become puzzling as other experiments have been performed. Thus, although the drop of the moment of inertia has been confirmed, crystal annealing was shown to lower dramatically the amplitude of this NCRI [8, 9]. Similarly, solid Helium submitted to pressure gradient could not flow except when large grain boundaries were present in the sample [10–12]. Moreover, the responses of solid ⁴He to a localized pressure jump presented no evidence of superflow in the solid[13, 14]. The experimental context presents thus apparent contradictions between NCRI measurements and pressure driven flows with the role of disorder (through vacancies, grain boundaries...) to be elucidated. On the other hand the theoretical framework for describing supersolids presents also fundamental puzzles (see the recent review of Prokof'ev[15] where the influence of the disorder is particularly discussed). Beside Penrose and Onsager argument[16], Monte-Carlo models claim that a perfect crystal cannot exhibit supersolid behavior[17, 18]. However, the account for exchange processes between neighboring atoms [3, 19], the densities and the role of the vacancies in the dynamics raise still fundamental questions on the existence and the nature of the supersolidity (see [20, 21] for instance).

An alternative issue consists of using the Gross-

Pitaevskii (GP) model[22] to describe the dynamics of a quantum solid, as proposed in 1994 by Pomeau and Rica[23]. The original GP equation[22] is used, with a roton minimum in the dispersion relation, where the ground state exhibits a first order phase transition to a crystalline state. However, the assumptions underlying the GP equation are not strictly speaking valid for Helium although this equation is believed to give a good qualitative description of superfluid Helium. Therefore this model, even crude in its basic structure, is at least a good testbed for theories of supersolids, that are still in a state of uncertainty. In Ref. [24, 25], two of us have developped the theory for the long wave perturbations of this model of supersolid and we have shown that this model was able to conciliate the apparent experimental contradiction discussed above. In the present paper, we study the one-dimensional (1D) version of this model. Beside the simplicity of the 1D approach, which then allows precise determination of the crystal structure, the 1D limit is particularly interesting since it can model to some extent an annular geometry.

THE MODEL

The starting point is the original GP equation[22] for the complex wavefunction $\psi(x, t)$ in one space dimension:

$$i\hbar \frac{\partial \psi}{\partial t} = -\frac{\hbar^2}{2m} \frac{\partial^2 \psi}{\partial x^2} + \psi \int_{-\infty}^{\infty} U(|x-y|) |\psi(y)|^2 dy, \quad (1)$$

where $U(s)$ is the two body potential depending on the relative distance. The potential $U(s)$ should satisfy

$$0 < \int_{-\infty}^{\infty} U(s) ds < \infty,$$

for stability and its Fourier transform:

$$\hat{U}_k = \int_{-\infty}^{\infty} U(s) e^{iks} ds \quad (2)$$

has to be bounded for all k . Moreover, as we will see later, we shall require also that the Fourier transform \hat{U}_k

becomes negative at some k_c to allow roton crystallization.

This dynamics conserves the Hamiltonian (or the energy, following $\partial_t \psi = \frac{\delta H}{\delta \psi^*}$)

$$H = \frac{\hbar^2}{2m} \int_{-\infty}^{\infty} |\partial_x \psi|^2 dx + \frac{1}{2} \int_{-\infty}^{\infty} \int_{-\infty}^{\infty} U(|x-y|) |\psi(y)|^2 |\psi(x)|^2 dy dx, \quad i \frac{\partial \psi}{\partial t} = -\frac{1}{2} \frac{\partial^2 \psi}{\partial x^2} + \frac{\Lambda}{2} \psi(x, t) \int_{x-1}^{x+1} |\psi(y)|^2 dy. \quad (4)$$

the number of particles

$$N = \int_{-\infty}^{\infty} |\psi(x)|^2 dx$$

and the linear momentum

$$P = -\frac{i\hbar}{2} \int_{-\infty}^{\infty} (\psi^* \partial_x \psi - \psi \partial_x \psi^*) dx.$$

According to the energy, the ground-state solution is real since any non uniform phase increases its energy.

The dynamics exhibits indeed an homogenous and stationary solution $\psi_0 = \sqrt{n_0} e^{-i \frac{E_0}{\hbar} t}$, with n_0 the mean 1D density and $E_0 = n_0 \int_{-\infty}^{\infty} U(s) ds$. This solution is stable and can also be the ground state for small enough n_0 as suggested by the Bogoliubov spectrum of the perturbations[26] (see below):

$$\hbar \omega_k = \sqrt{(\hbar^2 k^2 / 2m)^2 + (\hbar^2 k^2 / m) n \hat{U}_k}$$

Assuming that the potential scales like U_0 and possesses a single length scale a , the spectrum depends then only on a single dimensionless parameter[23]:

$$\Lambda = n_0 \frac{ma^2}{\hbar^2} \hat{U}_0,$$

with $\hat{U}_0 = \int_{-\infty}^{\infty} U(s) ds \sim U_0 a$. For some analytical results and for the numerics later on, we choose the soft core interaction, with no loss of generalities:

$$U(|x-y|) = U_0 \theta(a - |x-y|), \quad (3)$$

with $\theta(\cdot)$ the Heaviside function. The Fourier transform of this special interaction potential is

$$\hat{U}_k = 2U_0 \frac{\sin(ka)}{k} = \hat{U}_0 \frac{\sin(ka)}{k}.$$

It should also be noticed that the special choice of the potential (3) is purely of practical interest because it is easy to implement in some numerical schemes and can be easily used for variational estimates. Other functions whose fourier transform would be negative for a wavenumber domain (strictly bigger than zero), would show similar properties. Among them are the classical two bodies atomic potential with strong repulsion at short scale and a slight attraction for large scale or a potential \hat{U}_k choosen in such a way that the Bogoliubov dispersion relation matches the Landau spectrum with

the right values of the speed of sound c , and the three roton parameters[27].

With $x' = x/a$, $t' = \frac{ma^2}{\hbar} t$ and $\psi' = \sqrt{n_0} \psi$, the dimensionless GP equation for the Heaviside interaction (we drop the primes hereafter) reads:

Finally, we emphasize that an annular geometry can be simplified into a 1D system by considering periodic boundary condition $\psi(x, t) = \psi(x + L, t)$ (L is dimensionless) and by assuming that the transverse structure of the solid can be neglected. We then define the energy and number of particles densities:

$$\mathcal{E} = \frac{1}{2L} \int_0^L \left(|\psi_x|^2 + \frac{\Lambda}{2} |\psi|^2 \int_{x-1}^{x+1} |\psi(y)|^2 dy \right) dx, \quad (5)$$

$$\rho = n_0 = \frac{1}{L} \int_0^L |\psi(x, t)|^2 dx. \quad (6)$$

GROUND STATE

As shown in [23], for low Λ the ground state is a superfluid (without positional order). However above a critical value, Λ_c the ground state shows a periodic modulation of the density in space. Although in two and three space dimensions the transition is first order as Λ increases, it is supercritical (second order) in one space dimension[31]. The periodic structure arising from the instability can be analytically estimated through a variational approach for a fixed wavelength λ at least in two regimes: close to the transition and for large Λ .

If $\Lambda \gtrsim \Lambda_c$, a weak amplitude development of wavenumber k and normalized to unity reads:

$$\psi(x) = \frac{1}{\sqrt{1 + 2|A|^2}} (1 + A e^{ikx} + A^* e^{-ikx}). \quad (7)$$

Minimizing the energy of such solution gives:

$$|A|^2 = -\frac{k^2 + 4\Lambda \hat{U}_k / \hat{U}_0}{2(k^2 + \Lambda(\hat{U}_{2k} - 4\hat{U}_k) / \hat{U}_0)} \quad (8)$$

and the following wave-number selection $k_c a = 4.078 \dots$. The amplitude for this wave number k_c follows

$$|A_c|^2 = (\Lambda - \Lambda_c) \frac{-4\sin(k_c)}{4k_c(k_c^2 + \Lambda_c \cos^2(k_c)/3)}.$$

while for $k \sim k_c$, $|A_c|^2 - |A|^2 \propto (k - k_c)^2$.

In the large Λ limit, the density exhibits strongly nonlinear structures since the potential energy in (5) requires small ψ while the mass normalization (6) forbids ψ to be small every-where. Therefore the energy minimization

leads to a periodic structure with zones where $\psi \approx 0$ balancing zones where $\psi \gg 1$. In the $\Lambda \rightarrow \infty$ limit, Ref. [28] showed that $\psi \neq 0$ only in a small zone $x \in (-\delta, \delta)$ of the whole period $(0, \lambda)$. The Euler-Lagrange condition deduced from (5) together with (6) leads to the Hemholtz equation in the domain $(-\delta, \delta) : -\psi''(x) = \mu\psi$. Finally the minimization of the energy gives δ and the wave number λ of the periodic structure. Following this approach, we sketch now an estimate of the ground state for finite $\Lambda \gg 1$. We use the trial function for a single period:

$$\psi(x) = \sqrt{\frac{\lambda}{\delta}} \cos\left(\frac{\pi x}{2\delta}\right) \quad (9)$$

in $x \in [-\delta, \delta]$ and zero elsewhere, that satisfies exactly the normalization condition (6). Introducing this trial function into the energy (5), we obtain: $\mathcal{E} = \mathcal{E}_1 + \mathcal{E}_2 + \mathcal{E}_3$, with the kinetic energy

$$\mathcal{E}_1 = \frac{\pi^2}{8\delta^2},$$

the self interaction of a pulse with itself

$$\mathcal{E}_2 = \frac{\Lambda\lambda}{4},$$

and the nontrivial interaction of a pulse with its two near neighbors

$$\mathcal{E}_3 = \frac{\Lambda}{2} \int_{\lambda-1-\delta}^{\delta} \psi(x)^2 \int_{-\delta}^{x+1-\lambda} \psi(y)^2 dy dx.$$

This energy \mathcal{E}_3 is not zero only if $\lambda < 1 + 2\delta$ (and naturally, we have $\lambda > 2\delta$).

The energy \mathcal{E} may be understood as a function of δ and of the periodicity length λ . Then, the variation of total energy in the (δ, λ) plane shows the existence of a global minimum and a saddle for large enough Λ . As Λ decreases, the saddle and the global minimum collide, and we obtain a pure monotonic energy landscape in the (δ, λ) plane, leading to both λ and δ to infinity as minimizer. On the other hand, when $\Lambda \rightarrow \infty$ the global minimum moves to $(\delta, \lambda) \rightarrow (0, 1)$. This selection mechanism holds for an infinite domain where the wavelength λ can vary continuously. In a finite domain, λ can only take discrete values related to the number N_c of unitary cells, $\lambda = L/N_c$. Numerical simulations suggest also the existence of a large energy barrier between minimizers with different number of cells N_c for large Λ . Thus, for a given domain size L , the energy, as function of (δ, λ) , is now described by a discrete set of energy functions of δ for each available λ satisfying $\lambda = L/N_c$. One has now to minimize each energy with respect to δ . For small Λ (typically smaller than Λ_c) none of these functions have minima. For large Λ on the other hand, there is a finite band of λ for which the energy admits a minimum as δ varies. The minimization of this energy respect to δ

provides relations among δ and Λ with the wavelength λ as a fixed parameter. To determine the global minimum and to avoid further algebraic difficulties, we introduce the new variable: $z = \pi(\lambda - 1)/\delta$ where $0 \leq z \leq 2\pi$ for our problem (in particular, $z > 2\pi$ means that the peaks do not interact one with another). Minimizing the energy gives a relation for $\Lambda = \Lambda(\lambda, z)$:

$$\Lambda = \frac{4\pi^2 z}{\lambda(\lambda - 1)^2((2\pi - z)(\cos(z) + 2) + 3\sin(z))}. \quad (10)$$

Fig. 1 shows δ versus Λ for different values of λ . The analytical curves are shown together with the results of direct numerical simulations described below.

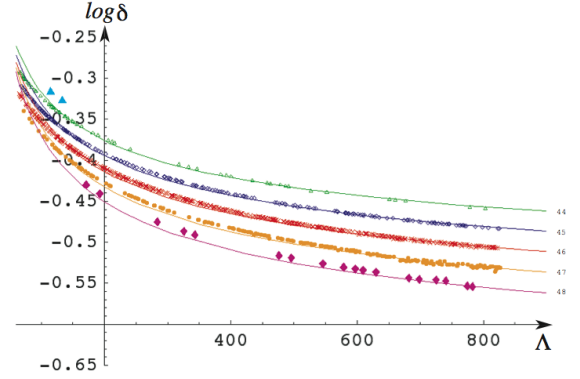


FIG. 1: Plot of $\log_{10}\delta$ as a function of Λ for different λ . The curves correspond to formula (10) while the points come from numerical simulations. The total size of the system is 64 units and the range of the interaction is $a = 16$. The system displays a number of cells varying from 44 to 48 (identified at the right hand side of the figure). The respective λ vary thus from $4/3$ to $16/11$.

Finally, an exponential “boundary layer” correction developps near $x = \pm\delta$ where the nonlinear term in eq. (4) cannot be neglected, as noticed by [28]. In the limit of large Λ , where similarly $\lambda \rightarrow 1$, the nonlinear term of eq. (4) gives near $x = \delta$:

$$\lim_{\lambda \rightarrow 1} \int_{x-1}^{x+1} \psi(y)^2 dx = Cte + \lim_{\lambda \rightarrow 1} \int_{\lambda-\delta}^{x+1} \psi(y)^2 dx \approx Cte + \frac{\pi^2}{12\delta^3} (x - \delta)^3.$$

The ground state is thus modified into $\psi(x) + \varphi(x)$, where $\psi(x)$ is the trial function (9), and φ satisfies a linear Schrödinger equation:

$$-\frac{1}{2}\varphi''(x) + \frac{\Lambda}{2}V(x)\varphi(x) = 0,$$

where the first nontrivial term for the potential reads $V(x) = \frac{\pi^2\lambda}{12\delta^3}(x - \delta)^3$. The solution may be computed directly in term of Bessel functions : $\varphi(x) =$

$K_*\sqrt{x}K_{1/5}\left(\frac{\pi}{5}\sqrt{\frac{\Lambda\lambda}{3\delta^3}}(x-\delta)^{5/2}\right)$. where the constant K_* results from the matching of the exponentially small boundary layer and the trial function. One can also expand this solution *via* a WKB approximation $\varphi(x) = K_*e^{-\sqrt{\Lambda}S(x)}$ with $S(x) = S_0(x) + \frac{1}{\sqrt{\Lambda}}S_1(x) + \dots$. We obtain then $S_0(x) = \int \sqrt{V(x)}dx$ and $S_1(x) = \frac{1}{2}\log(S'_0(x))$ and therefore

$$\varphi(x) = \frac{K_*}{\sqrt{S'_0(x)}}e^{-\sqrt{\Lambda}S_0(x)}$$

with $S_0(x) = \frac{\pi\sqrt{\lambda/3}}{5\delta^{3/2}}(x-\delta)^{5/2}$.

NON-CLASSICAL MOMENT OF INERTIA IN SUPERFLUIDS AND SUPERSOLIDS.

The precise estimation of the ground state is in fact crucial to describe the supersolid features of the model. Indeed, we have obtained in Refs. [24, 25], using the homogenization technique [29], an expression for the effective or superfluid density matrix ϱ_{ik}^{ss} deduced from the density profile of the crystal.

We shall in fact explore the low excited states around the ground state, described by the knowledge of the crystal density $\rho_0(x)$. The change of energy for phase variations gives:

$$\Delta E = \frac{1}{2} \int \rho_0(x) \left(\frac{\partial \phi}{\partial x} \right)^2 dx. \quad (11)$$

and ϕ is determined by minimizing ΔE , that correspo, the Euler-Lagrange condition:

$$\frac{\partial}{\partial x} \left(\rho_0(x) \frac{\partial \phi}{\partial x} \right) = 0. \quad (12)$$

under the appropriate boundary conditions. As shown by Leggett [3], for a periodic $\rho_0(x)$ under rotation, ΔE is lower than that of a rigid solid rotation, which indicates that superfluidity is present.

In Refs. [24, 25] we have obtained an expression for the energy variation in three space dimensions $\Delta E = \frac{\hbar^2}{2m} \int \varrho_{ik}^{ss} \partial_i \phi \partial_k \phi d^3x$, where ϱ_{ik}^{ss} is the effective or superfluid density matrix. It can be explicitly expressed using a solution of a partial differential equation in the unit cell V of the solid, following:

$$\begin{aligned} \varrho_{ik}^{ss} &= n\delta_{ik} - \varrho_{ik} \\ \varrho_{ik} &= \frac{1}{V} \int_V \rho_0(\mathbf{r}) \nabla K_i \cdot \nabla K_k d\mathbf{r}. \end{aligned} \quad (13)$$

The vector K_i is a periodic function in the unit cell V that is solution of $\nabla_i \rho_0 + \nabla \cdot (\rho_0 \nabla K_i) = 0$.

In one space dimension, we can in fact deduce the density ϱ^{ss} exactly. Indeed the formula (13) simplifies then

into one term $\varrho^{ss} = n - \frac{1}{\lambda} \int_0^\lambda \rho_0(x) (\partial_x K_x)^2 dx$ where $K_x(x)$ is a periodic function in the interval $[0, \lambda]$ solution of $\partial_x \rho_0 + \partial_x (\rho_0 \partial_x K_x) = 0$. Thus $\partial_x K_x(x) = -1 + \frac{c}{\rho_0(x)}$ where c is an integration constant. The periodic boundary condition $K_x(0) = K_x(\lambda)$ gives $c = \frac{1}{\frac{1}{\lambda} \int_0^\lambda \frac{1}{\rho_0(x)} dx}$. Finally, we find that in one dimension, the superfluid density writes:

$$\frac{1}{\varrho_{ss}} = \frac{1}{c} = \frac{1}{\lambda} \int_0^\lambda \frac{1}{\rho_0(x)} dx.$$

Thus, the theory of homogenization provides us an exact result for the special case of one space dimension, and the effective density (scalar in 1D) is then a kind of “harmonic” average of the density [29].

From this formula, the non classical rotational inertia fraction (NCRIF) ϱ^{ss}/ρ corresponds exactly to the upperbound quotient Q_0 proposed by Leggett [3], who also established the equivalence for 1D systems more recently [30]. Therefore, the NCRIF at low speed ($NCRIF_0$) reads:

$$\varrho^{ss}/\rho = Q_0 \equiv \frac{1}{\left(\frac{1}{\lambda} \int_0^\lambda \rho_0(x) dx \right) \left(\frac{1}{\lambda} \int_0^\lambda \frac{1}{\rho_0(x)} dx \right)}. \quad (14)$$

Remarks.

1. The Schwartz inequality[32] and $\rho_0(x) \geq 0$ gives $0 \leq Q_0 \leq 1$.

2. For finite energy, if the ground state vanishes at some point, the non-classical rotational inertia does as well. Indeed, if at some point x_* we have $\rho_0(x) \sim |x-x_*|^\alpha$ with $\alpha > 0$, then

$$\int_0^\lambda \frac{1}{\rho_0(x)} dx \approx \text{finite term} + \int_{x_*-\epsilon}^{x_*+\epsilon} |x-x_*|^{-\alpha} dx$$

and

$$Q_0 \approx \frac{1}{\text{finite term} + \frac{2}{1-\alpha} \epsilon^{1-\alpha}}.$$

Therefore if $0 < \alpha \leq 1$, Q_0 remains finite with $\epsilon \rightarrow 0$. However, as we have seen above, such a ground state would require an infinite amount of energy.

RESULTS

NCRIF in the weakly nonlinear limit.

The NCRIF in the limit of weak modulation may be computed directly from the trial function (7):

$$Q_0 = \frac{(1-4|A|^2)^{3/2}}{(1+2|A|^2)}, \quad (15)$$

where $|A|^2$ is evaluated at $k = k_c$. As $|A| \rightarrow 1/2$, the quotient Q_0 vanishes, because the wavefunction (7) vanishes at some point.

NCRIF in the limit $\Lambda \rightarrow \infty$.

For large Λ , since the ground state $\rho_0(x)$ decays exponentially, the contribution to the NCRIF (14) mainly comes from the large contribution of $1/\rho_0(x)$ in $x \in [\delta, \lambda/2]$. That is, after using the WKB approximation:

$$Q_0 \approx \frac{5}{4} K_*^2 e^{-\frac{\pi}{5} \sqrt{\frac{\Lambda \lambda}{3\delta^3}} (\lambda/2 - \delta)^{5/2}}. \quad (16)$$

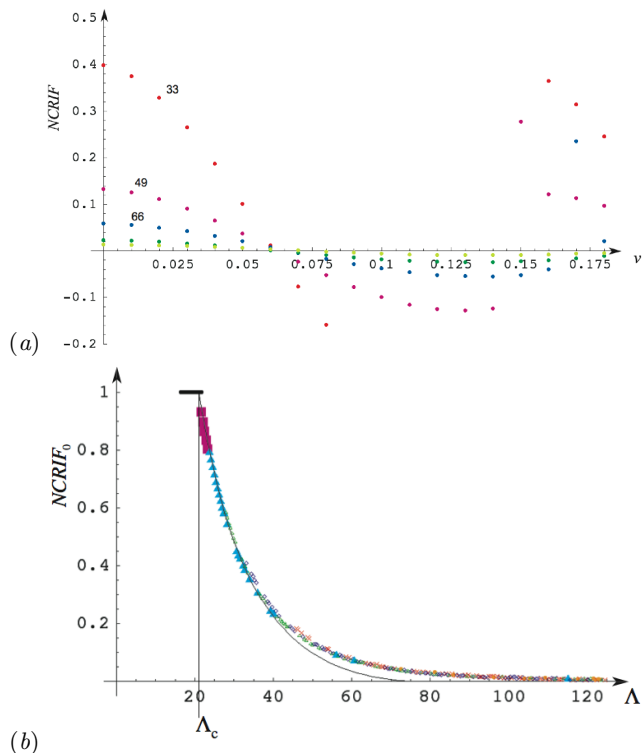


FIG. 2: (a) $NCRIF$ as a function of v for different values of Λ . (b) $NCRIF_0$ as a function of Λ , the line is the curve from the weakly non linear analysis, see formula (15) which gives a good approximation up to $\Lambda \approx 40$.

We will now be using numerical simulations to deduce the NCRI and compare it with theories by two different methods. First, the ground state is determined. Then, one can compute directly the NCRI by imposing a rotation to this ground state. On the other hand, the value of Q_0 can be calculated from the ground state solution $\rho_0(x)$.

Numerical results are obtained by minimizing the energy (5) under the number of particles condition (6). We use therefore the Ginzburg-Landau version of the dynamics which can be interpreted as the integration of the GP equation for imaginary time $t = -i\tau$:

$$\frac{\partial \psi}{\partial \tau} = \mu \psi + \frac{1}{2} \frac{\partial^2 \psi}{\partial x^2} - \frac{\Lambda}{2} \psi(x, t) \int_{x-1}^{x+1} |\psi(y)|^2 dy, \quad (17)$$

μ is the Lagrangian multiplier introduced to satisfy the number of particles condition.

Imposing a rotational frequency ω in a 1D annular system amounts to consider a drift of the system at constant velocity $v = \omega L$ with periodic boundary conditions. The ground state of such a system is obtained by minimizing: $\mathcal{F} = \mathcal{E} + v\mathcal{P} + \mu(N - n_0)$, where $\mathcal{P} = -\frac{i}{2L} \int_0^L (\psi^*(x) \partial_x \psi(x) - \psi(x) \partial_x \psi^*(x)) dx$. Consequently, a direct computation of the NCRIF can be performed numerically:

$$NCRIF(v) = 1 - \frac{|\mathcal{P}'(v)|}{\int_0^L |\psi(x)|^2 dx}.$$

Fig. 2(a) shows the function $NCRIF(v)$ for different Λ obtained by numerical minimization of \mathcal{F} . As expected, the NCRIF decreases as v increases. For large value of the parameter v , the NCRIF first become negatives and then show large fluctuations, indicating that complex structures are present, such as 2π phase jumps for instance (similar to vortices in higher dimensions). Moreover, numerical instabilities are also enhanced by the rotation so that only moderate Λ (up to 150) values could be achieved with full confidence.

The low speed limit:

$$NCRIF_0 = \lim_{v \rightarrow 0} NCRIF(v)$$

is then shown on Fig. 2(b) as function of Λ and compared with the analytical quotient (15) of the weak amplitude modulations, showing an excellent agreement.

On the other hand, as explained above, the $NCRIF_0$ can be calculated directly from the numerical solution $\rho_0(x)$, by computing the Leggett quotient Q_0 (14). Since the ground state solution is numerically more stable to obtain than the minimization of the rotating system, we are able to compute a satisfactory good estimates for Q_0 up to Λ of the order of 800, as shown on Fig. 3(a). Remarkably Q_0 does not depend on the wavelength of the periodic structure λ , since all the numerical data for different λ gather on a single curve. This is a consequence that the main contribution to the quotient Q_0 comes from the wide region with small values of $\rho_0(x)$. On the other hand, only poor agreement is found with the asymptotic behavior (16).

In Fig. 3(b) we compare this quotient Q_0 with the $NCRIF_0$ obtained by direct numerical simulation of the rotating system for the accessible moderate Λ values. It shows a particularly good numerical agreement between the two methods, as expected by the theory.

In conclusion, we have exhibited NCRI in a 1D model of supersolid in the context of annular geometry, using both direct numerical simulation and analytical estimates. In particular, we have shown that the so-called Leggett quotient was there in full agreement with NCRI. C.J. acknowledges the financial support of the DGA for this research and this research was supported in part by the National Science Foundation under Grant No.

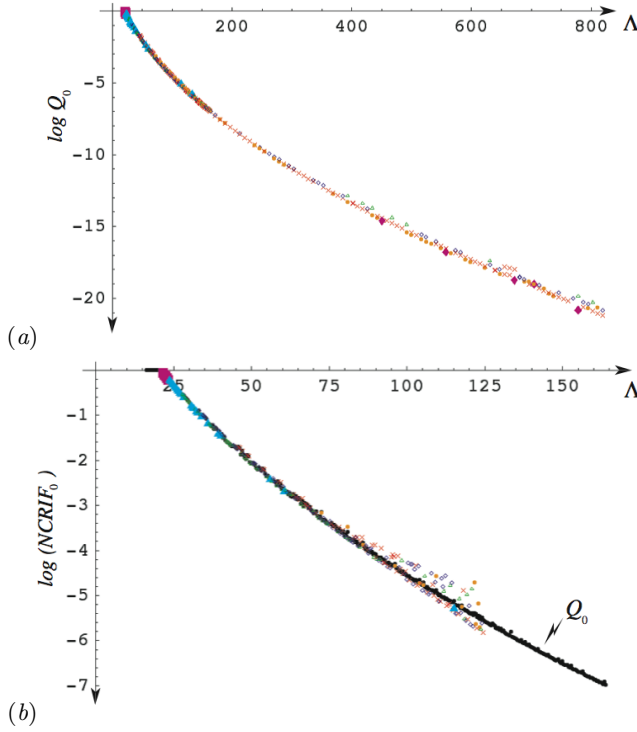


FIG. 3: (a) The quotient Q_0 as a function of Λ , using a direct numerical integration of ground states $\rho_0(x)$ obtained for Fig. 1. The lines are the functions obtained from the theory (16) for three different wavelength (similar notations as Fig. 1) with $K_* = 0.01$ as a fixed parameter. Notice the exponential behavior in qualitative agreement with (16). (b) Comparison between the numerical calculations $NCRIF_0$ and the Leggett's quotient Q_0 represented with black dots.

PHY05-51164. S.R. acknowledges Anillo de Investigación Act. 15 (Chile).

-
- [1] A.F. Andreev and I.M. Lifshitz, Sov. Phys. JETP. **29**, 1107 (1969).
 - [2] G.V. Chester, Phys. Rev., **A 2**, 256 (1970).
 - [3] A.J. Leggett, Phys. Rev. Letters, **25**, 1543 (1970).
 - [4] M.W. Meisel, Physica (Amsterdam) **178B**, 121 (1992).
 - [5] E. Kim and M.H.W. Chan, Nature (London) **427**, 225

- (2004).
- [6] E. Kim and M.H.W. Chan, Science **305**, 1941 (2004).
- [7] E. Kim and M.H.W. Chan, Phys. Rev. Lett. **97**, 115302 (2006).
- [8] A.S. Rittner and J.D. Reppy, Phys. Rev. Lett. **97**, 165301 (2006).
- [9] A.S. Rittner and J.D. Reppy, Phys. Rev. Lett. **98**, 175302 (2007).
- [10] D. S. Greywall, Phys. Rev. **B 16**, 1291 (1977).
- [11] G. Bonfait, H. Godfrin, B. Castaing, J. Phys. (Paris) **50**, 1997 (1989).
- [12] S. Sasaki, R. Ishiguro, F. Caupin, H.J. Maris and S. Balibar, Science **313**, 1098 (2006).
- [13] J. Day, T. Herman and J. Beamish, Phys. Rev. Lett. **95**, 035301 (2005).
- [14] J. Day and J. Beamish, Phys. Rev. Lett. **96**, 105304 (2006).
- [15] N. Prokof'ev, Advances in Physics **56**, 381 (2007).
- [16] O. Penrose and L. Onsager, Phys. Rev. **104**, 576 (1956).
- [17] D.M. Ceperley and B. Bernu, Phys. Rev. Lett. **93**, 155303 (2004).
- [18] N. Prokof'ev and B. Svistunov, Phys. Rev. Lett. **94**, 155302 (2005).
- [19] A.J. Leggett, Science **305**, 1921 (2004).
- [20] P.W. Anderson, W.F. Brinkman and D.A. Huse, Science **310**, 1164 (2005).
- [21] D.E. Galli, M. Rossi and L. Reatto, Phys. Rev. B **71**, 140506(R) (2005).
- [22] L.P. Pitaevskii, Sov. Phys. JETP **13**, 451 (1961); E.P. Gross, J. Math. Phys. **4**, 195 (1963).
- [23] Y. Pomeau and S. Rica, Phys. Rev. Lett. **72**, 2426 (1994).
- [24] C. Josserand, Y. Pomeau and S. Rica, Phys. Rev. Lett. **98**, 195301 (2007).
- [25] Euro. Phys. J. S.T. **146**, 47-62 (2007).
- [26] N.N. Bogoliubov, J. Phys. USSR **11**, 23 (1947).
- [27] L.D. Landau, J. Phys. USSR **5**, 71 (1941).
- [28] A. Aftalion, X. Blanc and R.L. Jerrard, Phys. rev. Lett. **99**, 135301 (2007).
- [29] A. Bensoussan, J.L. Lions, and G. Papanicolaou, *Asymptotic Analysis in Periodic Structures*, North-Holland Amsterdam (1978).
- [30] A.J. Leggett, J. Stat. Phys. , **93**, 927 (1998).
- [31] With the potential constructed in (3) the critical value is $\Lambda_c = 21.05 \dots$
- [32] This inequality reads: $\left(\int_0^\lambda f(x)^2 dx \right) \left(\int_0^\lambda g(x)^2 dx \right) \geq \left(\int_0^\lambda f(x)g(x) dx \right)^2$.